

Validation of Time-Resolved Microwave Conductivity (TRMC) as a screening tool for all-polymer solar cells

Supriya Pillai,^a Neil Anderson,^a Chao Wang,^b Jonas M. Bjuggren,^c Martyn Jevric,^c Mats. R. Andersson,^c Nikos Kopidakis,^a and Christopher R. McNeill^c

^a School of Engineering, Macquarie University, Waterloo Road, Macquarie Park, NSW 2113, Australia

^b Materials Science and Engineering, Monash University, Wellington Road, Clayton, VIC 3800, Australia

^c Flinders Centre for Nanoscale Science and Technology, Flinders University, Sturt Road, Bedford Park, Adelaide, SA 5042, Australia

24th June 2019

Key words: All-polymer solar cells, Time-resolved microwave conductivity

Summary of Key Findings

The short circuit current of all-polymer solar cells measured under simulated sunlight is found to be strongly correlated with the time resolve microwave conductivity (TRMC) response of active layer films on quartz substrates. This outcome validates the use of TRMC to rapidly screen promising new all-polymer systems. A minimum $\phi\Sigma\mu$ peak signal of 0.06 cm²/Vs is proposed as being required before further optimisation of new systems in device geometries. Furthermore, the TRMC response of three new all-polymer solar cell systems is presented, with short-circuit currents realised in solar cells consistent with the peak signals measured with TRMC.

Introduction

Polymer solar cells are coming closer to commercialisation boosted by recent improvements in the efficiency of single junction cells beyond 15%.^{1,2} Polymer solar cells utilise a donor and acceptor material in order to effect efficient exciton dissociation.³ While polymer solar cells generally use a semiconducting polymer as donor material,⁴ different classes of materials can be used as the acceptor, including fullerene derivatives,³ semiconducting polymers⁵ and so-called small molecule non-fullerene acceptors.⁶ While fullerene derivatives were used for many years to realise the most efficient cells, non-fullerene acceptors have taken over as the most efficient acceptor class.⁶ Although efficiency is an important parameter, for commercialisation other factors are important including processability, stability and mechanical flexibility.⁷ Using semiconducting polymers for both donor and acceptor materials – for “all-polymer” solar cells – has a number of attractions including greater control over solution viscosity (important for roll-to-roll printing), superior mechanical flexibility, and greater thermal stability.⁷ Compared to blends between a polymer and small molecule, all-polymer blends are inherently more stable due to lower crystallinity of polymers and the entanglement of polymer chains in a blend that hinders demixing. However the record efficiency for all-polymer solar cells is ~ 11% requiring efficiency improvements to be commercially viable.

Key to the recent improvement in polymer solar cell efficiency has been the development of new materials, be they donor polymers or acceptor materials. A key advantage of organic semiconductors is the limitless variety of materials that can be synthesised. A disadvantage is that a lot of trial and error is involved in the screening of new materials. Since a predictive approach to organic solar cells is still far off, techniques that can reduce the time required to screen new materials are particularly attractive. One such technique is time-resolved microwave conductivity (TRMC), which is a pump-probe technique to measure the photoconductance of an active layer.⁸

Instead of having to make a complete device, which requires the optimisation of active layer thickness, the deposition of contact, encapsulation and testing, TRMC in principle can assess the potential efficiency of a novel donor/acceptor system by quickly measuring the transient photoconductivity of a thin film prepared on a quartz substrate. By screening for systems with the highest photoconductivity and longest carrier lifetimes – which have been positively correlated with the short-circuit current of a device under simulated sunlight – significant time and cost in device fabrication and characterisation can be saved.⁹ While this approach has been successfully employed for the study and screening of polymer:fullerene systems,⁹ this approach has not been validated for systems based on other acceptor materials. This report investigates the feasibility of using TRMC to screen for efficient all-polymer systems, by comparing the TRMC response of a range of all-polymer systems to their photovoltaic performance.

Methodology

Materials

Figures 1 and 2 present the chemical structures of the donor and acceptor materials used in this study. A range of previously published systems have been selected with efficiencies spanning from less than 1%¹⁰ to over 7%.¹¹ Rather than relying on literature published values of efficiency, short-circuit current, open circuit voltage and fill factor, devices were fabricated and characterised to be able to directly compare the TRMC response of films on quartz substrates and active layer films in devices.

Most of the polymers used were sourced commercially. P3HT was sourced from Rieke Metals. PTB7, PTB7-Th, J51, J52, F-N2200 were purchased from 1-Material Inc. N2200 (also known as P(NDI2OD-T2)) was purchased from Raynergy Tech. S2-N2200 was provided by the group of Prof. Michael Sommer (Chemnitz University of Technology) while PNDI-T10 was synthesised in-house at Flinders University.

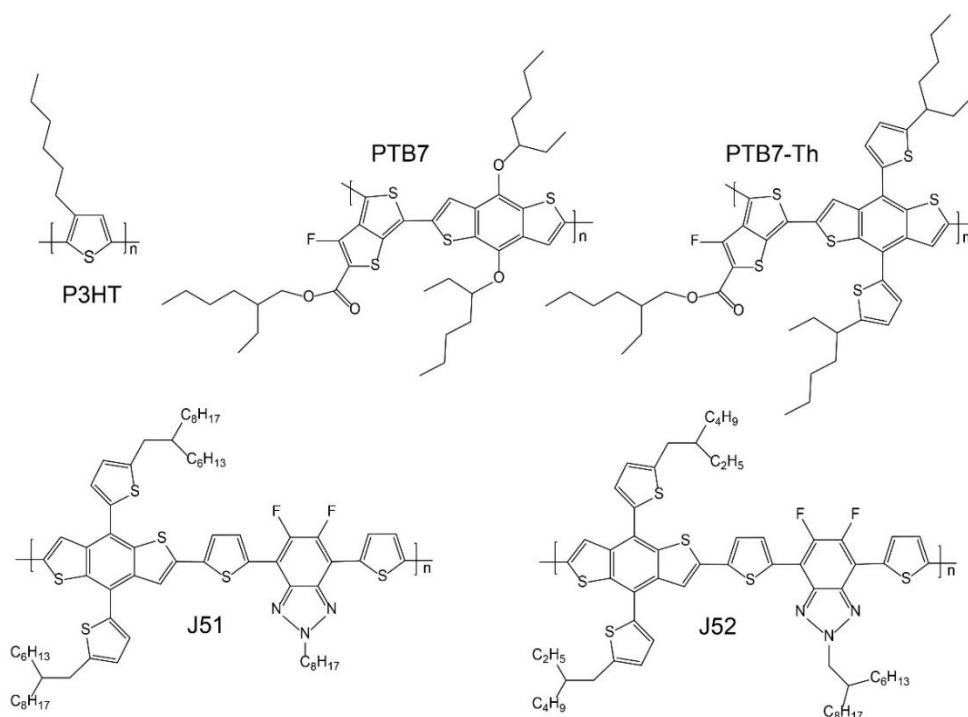


Figure 1. Chemical structures of donor polymers used in this study.

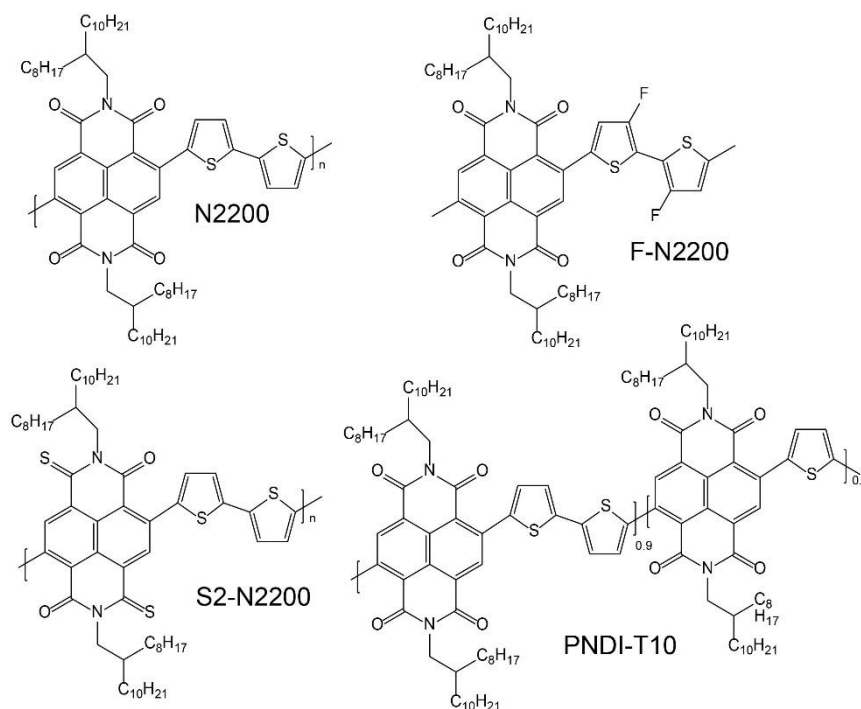


Figure 2. Chemical structures of acceptor polymers used in this study.

Device fabrication and characterisation

Solar cells were fabricated with an inverted architecture: ITO/ZnO/PEIE/active layer/MoO_x/Ag. ITO-coated glass substrates were cleaned firstly by sonication for 10 minutes in acetone, followed by sonication for another 10 minutes in isopropanol before oxygen plasma cleaning for 10 minutes. A 0.1 M ZnO precursor solution was prepared by dissolving 160 mg of zinc acetate dehydrate in 61 mg of ethanolamine and 10 mL of 2-methoxyethanol with vigorous stirring for 12 hours for the hydrolysis reaction at 60 °C. A 0.073 M ZnO precursor solution was then spin-coated onto cleaned ITO-coated glass at 3000 rpm for 30 s and annealed on a hot plate at 200 °C for 30 minutes to form a thin conducting layer. A PEIE layer was subsequently spin coated on top of the ZnO layer at 5000 rpm for 30 s and annealed on a hot plate at 110 °C for 15 mins to form a thin hole-blocking layer. The active layers of the solar cells were spin coated from blend solutions at different spin speed for 60 s. Finally, a 15 nm MoO_x layer with a 100 nm Ag layer was thermally deposited. All top electrode layers were deposited via thermal evaporation in vacuo ($\sim 10^{-6}$ mbar) through a shadow mask to define electrodes with an active area of 4.5 mm². Devices were encapsulated with epoxy resin and glass cover slides before being moved from the glove box for testing. Current–voltage (J–V) characteristics for all devices were measured using a Keithley 2635 source meter. A Photo Emission Tech model SS50AAA solar simulator, simulating an AM1.5G radiation spectrum with 100 mW/cm² irradiance, was used. The intensity of the simulator was calibrated with a silicon reference cell with a KG3 glass filter. External quantum efficiency (EQE) was measured using a spot size smaller than that of the device active area. An Oriel Cornerstone 130 monochromator was used to disperse light from a tungsten filament (Newport 250 W QTH). Prior to measurement, this system was calibrated using a Thorlabs FDS-100CAL photodiode placed at the exact location of the devices during measurements.

Time-resolved microwave conductivity measurements

Samples for TRMC were prepared on quartz substrates. The same weight ratio and casting solvent was used, with thickness altered where necessary to increase the optical density at the probe wavelength to at least 0.7. A photograph of the TRMC setup is shown in Figure 3. The sample under test is placed in the resonance cavity of an X-band microwave waveguide, which is located within the laser enclosure. Within the laser enclosure, a 5 ns pulse from a Nd:YAG laser is used to excite the carriers, with microwaves used to probe the relative population of the excited carriers. A wavelength of 532 nm is used with a frequency of 10 Hz. The relative change in the absorbed microwave power (provided by a custom-built source driven by a Voltage Control Oscillator (VCO) from Sivers IMA) from the dark signal to the excited signal, is directly proportional to the photoconductance ΔG :

$$\Delta G = \beta q_e I_0 F_A (\phi \Sigma \mu) \tag{1}$$

The product $\phi \Sigma \mu$, which is the product of the quantum yield and sum of the mobilities of the electrons and holes, is the figure of merit extracted from the TRMC measurements. All other parameters are measurable quantities. β is the geometric factor for the X-band waveguide ($\beta=2.2$ (W/H)), q_e is the elementary charge, I_0 the incident photon flux from the laser excitation and F_A is the fraction of light absorbed at the excitation wavelength which in our case is 532 nm. ΔG decays with time related to the lifetime of the excited charges, with the transient microwave photoconductivity recorded using a digital oscilloscope (Keysight).

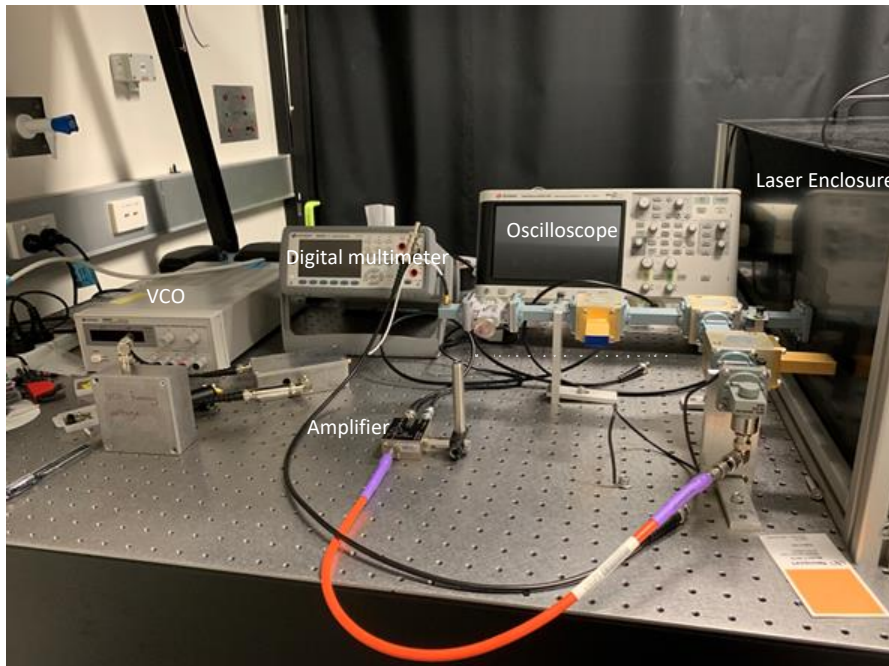


Figure 3. Photograph of the TRMC setup at Macquarie University used in this study.

Results

Table 1 summarises the solar cell performance of the eight all-polymer systems studied. The power conversion efficiencies of these systems ranges from $\sim 0.5\%$ to over 7% , with J_{sc} ranging from ~ 2 mA/cm² to ~ 14 mA/cm². P3HT:N2200 was chosen as being representative of earlier, low efficiency systems. The efficiency of the P3HT:N2200 is known to be limited by coarse phase

separation and geminate recombination.¹⁰ Replacing the donor polymer P3HT for either PTB7 or PTB7-Th results in a significant improvement in cell performance to 2.2% and 4.5% respectively. The PTB7:N2200 and PTB7-Th:N2200 systems are also interesting since the small difference in side chain in PTB7 compared to PTB7-Th results in a doubling of efficiency.¹² A subtle change in the chemical structure of the acceptor polymer switching N2200 for PNDI-T10 can also produce a significant increase in efficiency, with literature values of over 7% reported,¹³ although in our hands a more modest efficiency of ~5% was realised. Small changes in the chemical of N2200 can also have a detrimental effect with the thionation of N2200 to produce 2S-N2200 causing a reduction in efficiency from 4.5% to 0.8%.¹⁴ The highest efficiencies are realised with J51 and J52 as donor in combination with N2200, with an efficiency of 5.7% achieved for the J51:N2200 blend and 7.3% for the J52:N2200 blend. A J52:F-N2200 blends is also included, with fluorination resulting in a decrease in efficiency mainly due to a decrease in open circuit voltage, with short circuit current remaining relatively high.

Table 1. Summary of the solar cell performance of the eight all-polymer systems studied.

System	Weight ratio	Casting solvent	PCE (%)	V _{oc} (V)	J _{sc} (mA/cm ²)	FF
P3HT:N2200	1:1	Chloroform	0.53	0.55	1.7	0.57
PTB7:N2200	1:1	Chlorobenzene	2.2	0.77	7.3	0.40
PTB7-Th:N2200	1:1	Chlorobenzene	4.5	0.79	11.7	0.48
PTB7-Th:PNDI-T10	1:1	Chlorobenzene	5.0	0.81	12.6	0.49
PTB7-Th:S2-N2200	1:1	Chlorobenzene	0.8	0.49	5.2	0.33
J51:N2200	1:1	Chlorobenzene	5.7	0.81	13.9	0.51
J52:N2200	1:1	Chlorobenzene	7.3	0.81	14.4	0.62
J52:F-N2200	1:1	Chlorobenzene	4.7	0.69	12.4	0.55

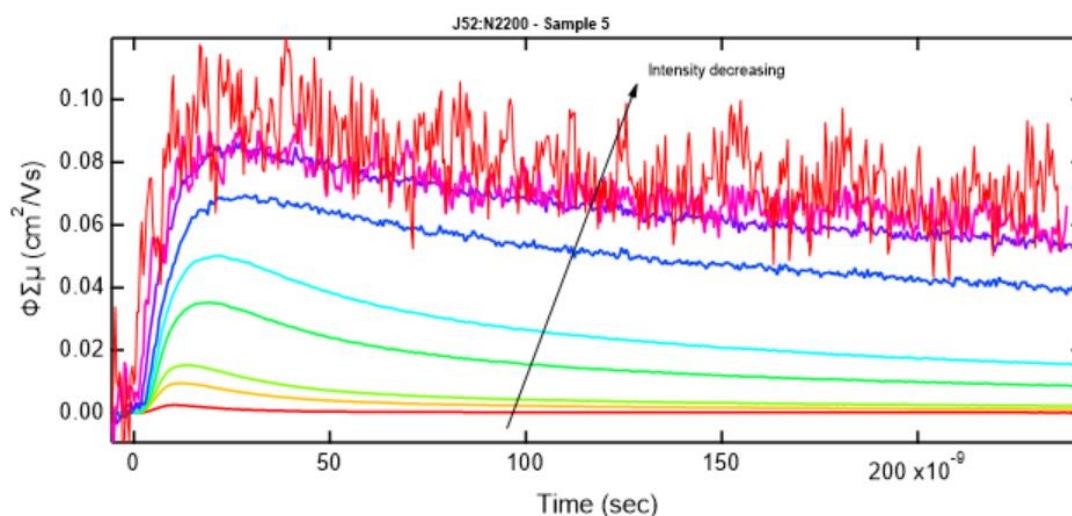


Figure 4. TRMC traces taken of a J52:N2200 film as a function of photon flux density, varied using neutral density filters with optical density varying from 0 to 4.3.

Figure 4 presents example TRMC traces recorded of the J52:N2200 sample. This plot shows the transient response as a function of laser pulse intensity. As $\phi\Sigma\mu$ is normalised to laser intensity, at high pulse intensity, the product $\phi\Sigma\mu$ decreases in absolute value above a certain threshold due to bimolecular recombination, with a corresponding decrease in lifetime (faster decay of $\phi\Sigma\mu$). Measurements were performed such that the peak $\phi\Sigma\mu$ figure of merit (the highest value of $\phi\Sigma\mu$ that the trace reaches) was taken from the linear regime at laser intensities low enough such that the traces were not affected by the bimolecular recombination of charges.

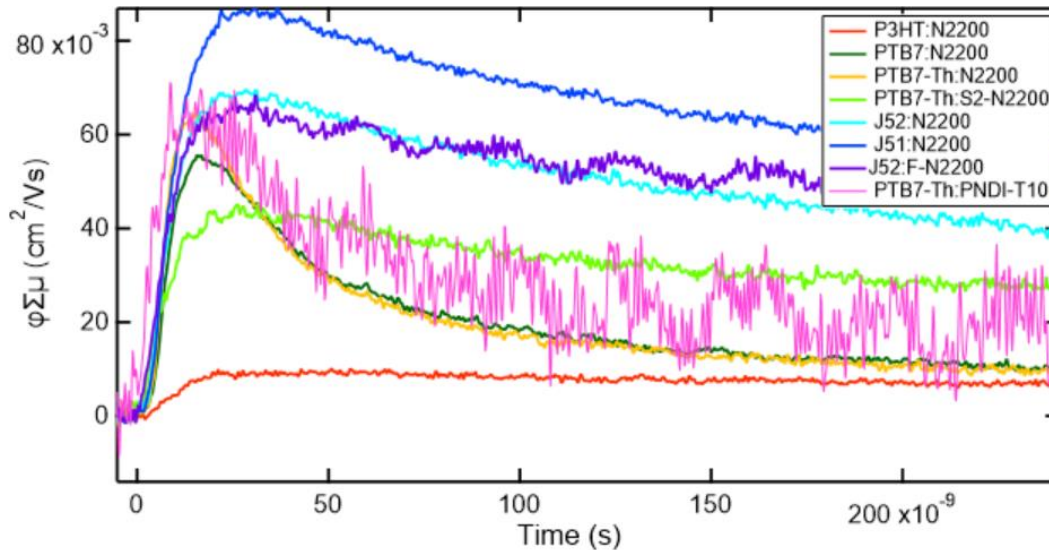


Figure 5. TRMC traces of the 8 all-polymer blend systems studied, with all traces recorded in the linear regime.

Figure 5 presents representative TRMC traces of the 8 all-polymer systems studied. These traces were recorded in the linear regime. From these traces the TRMC figure of merit was extracted as the highest value of $\phi\Sigma\mu$ attained.

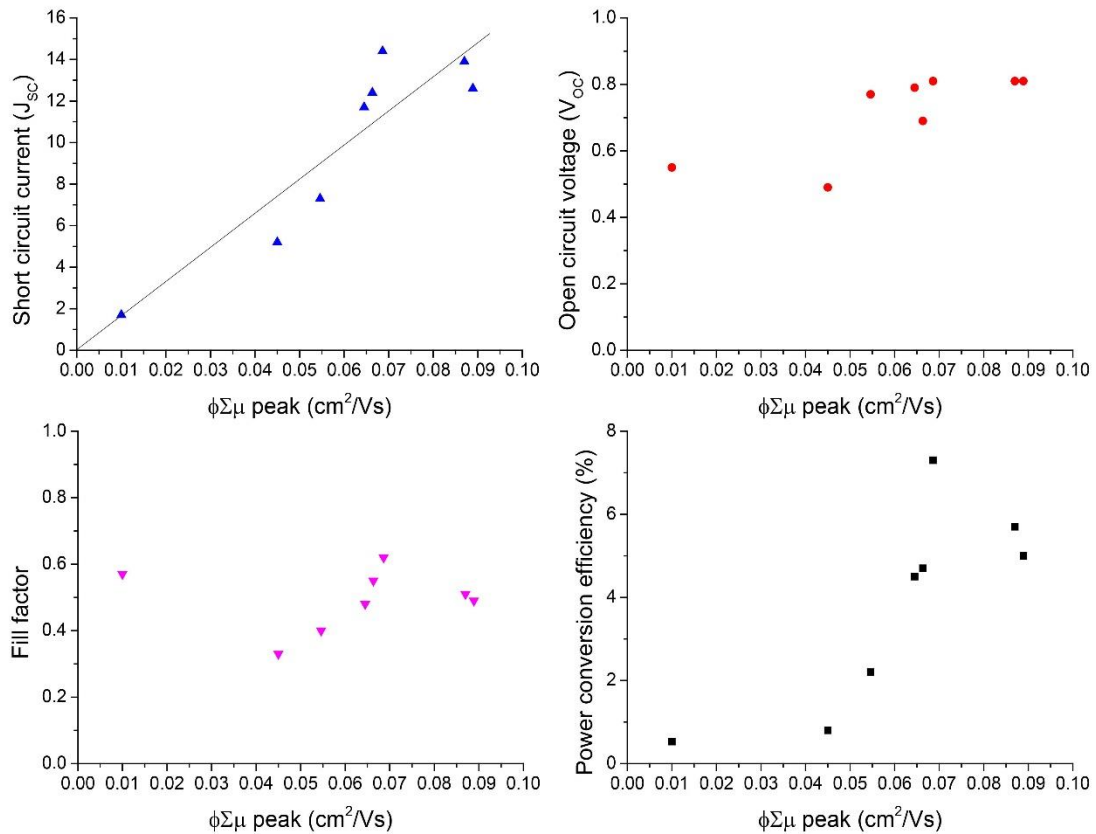


Figure 6. Comparison between various photovoltaic performance parameters and the TRMC $\phi\Sigma\mu$ peak figure of merit.

Figure 6 provides a comparison between the TRMC $\phi\Sigma\mu$ peak figure of merit and various photovoltaic performance parameters. As seen for polymer:fullerene systems, there is a strong correlation between the measured $\phi\Sigma\mu$ peak and short circuit current, figure 6(a), confirming for all polymer systems that a strong TRMC signal is positively correlated with the short circuit current measured in a device under simulated sunlight. For open circuit voltage and fill factor there is not as strong a correlation with the measured $\phi\Sigma\mu$ peak. Indeed, one of the highest fill factors was achieved for the cell with the lowest the $\phi\Sigma\mu$ signal (P3HT:N2200). For the P3HT:N2200 system this can be understood in terms of the high geminate recombination in this system;¹⁰ those carriers that are able to separate from the donor:acceptor interface are collected with low subsequent recombination due to the high mobilities of the P3HT and N2200 phases. Indeed, the decay of the TRMC signal of the P3HT:N2200 sample is noticeably slower than that of the other blends suggesting the FF may be correlated with TRMC lifetime. The open circuit voltage measured was in general found to be higher for systems with larger $\phi\Sigma\mu$ signal but tended to saturate for values of $\phi\Sigma\mu$ above 0.05 cm²/Vs. The additional scatter in the correlation between FF, V_{oc} with $\phi\Sigma\mu$ peak mean that the correlation between power conversion efficiency and $\phi\Sigma\mu$ peak is not as strong as between short circuit current and $\phi\Sigma\mu$ peak, however there is still a strong positive correlation. In general the data of figure 6 validate the use of TRMC for screening new all polymer systems. A threshold value of 0.06 cm²/Vs could be considered for screening new materials, with a strong preference for high efficiency systems (PCE > 5%). Due to the poorer correlation between $\phi\Sigma\mu$ peak and cell fill factor and open circuit voltage, other material factors such as charge carrier mobility and complementary energy

levels could be considered when selecting material combinations for TRMC screening, or when selecting between material combinations that have passed TRMC screening for device optimisation.

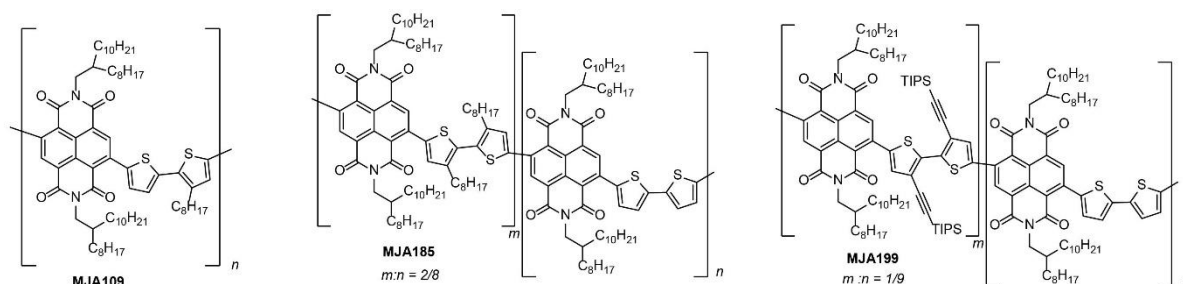


Figure 7. Chemical structures of three new acceptor polymers developed at Flinders University, MJA109, MJA185, MJA199.

To further explore the potential for TRMC for screening materials, we have also investigated three new all-polymer blends, based on three new acceptor polymers synthesised at Flinders University, see figure 7. MJA109, MJA185, MJA199 are variants of N2200 where novel sidechains have been added to the thiophene rings in order to tune aggregation and crystallisation behaviour. The acceptor polymers were combined with the donor J52. Table 2 presents the solar cell performance of optimised J52:MJA109, J52:MJA185, and J52:MJA199 solar cells, using the same device geometry as described above. The J52:MJA109 and J52:MJA185 systems are able to achieve efficiencies of $\sim 5\%$ with J_{SC} above 10 mA/cm^2 . J52:MJA199 was only able to achieve an efficiency of $\sim 2\%$ due to its lower V_{OC} and FF, with a J_{SC} of $\sim 10 \text{ mA/cm}^2$ still achievable.

Table 2. Summary of the solar cell performance of three new all-polymer systems.

System	Weight ratio	Casting solvent	PCE (%)	V_{OC} (V)	J_{SC} (mA/cm^2)	FF
J52:MJA109	1:1	Chlorobenzene	5.3	0.85	12.2	0.51
J52:MJA185	1:1	Chlorobenzene	5.0	0.83	10.5	0.57
J52:MJA199	1:1	Chlorobenzene	2.0	0.57	9.77	0.36

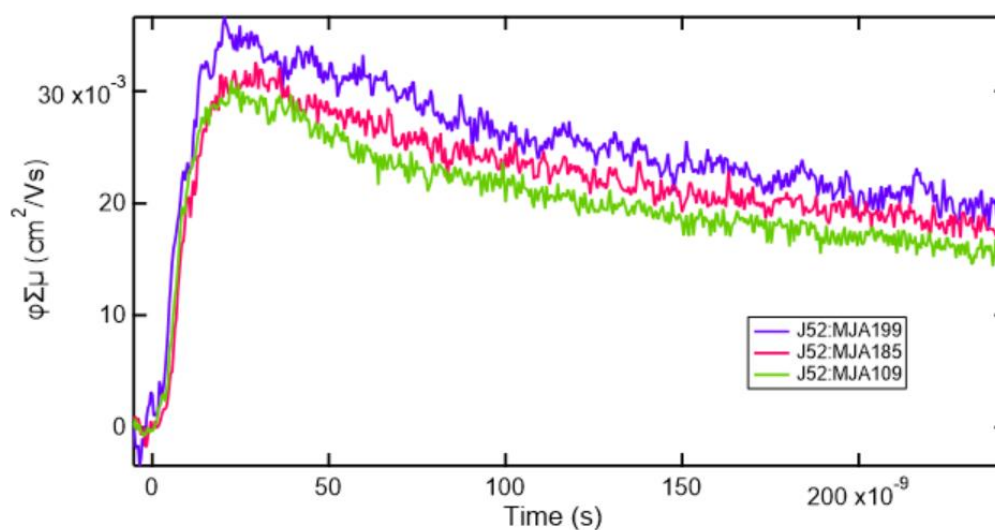


Figure 8. TRMC traces of three new all-polymer systems, J52:MJA109, J52:MJA185 and J52:MJA199.

Figure 8 presents TRMC traces of J52:MJA109, J52:MJA185, and J52:MJA199 films. Interestingly all systems show similar traces. With similar $\phi\Sigma\mu$ peak values of $\sim 30 \times 10^{-3} \text{ cm}^2/\text{Vs}$. The similar $\phi\Sigma\mu$ peak values agree with the similar J_{sc} values measured for the samples. The lower overall efficiency of the J52:MJA199 system must be attributed to other factors such as mismatched energy levels which lead to a lower V_{oc} .

To further analyse the transient response of these three new systems, transient responses were fitted using a double exponential decay fit:

$$y = A_1 \exp(-inv\tau_1 \cdot x) + A_2 \exp(-inv\tau_2 \cdot x)$$

The fits allow the qualitative comparison of free carrier lifetime for the samples. The transients were measured over an intensity range of absorbed photons across more than three orders of magnitude. The transients are analysed using two lifetime characters, τ_1 and τ_2 and their respective amplitudes denoted by A_1 and A_2 . In the decay curve, τ_1 denotes the slow component and τ_2 the fast component. Figure 9 shows the plots for τ_1 and τ_2 for three new systems. The corresponding plots for A_1 and A_2 can be found in figure 10. It can be seen that as the intensity is lowered, the lifetime becomes longer, due a decrease in second order recombination losses. Ideally longer the charges live better the carrier extraction in devices. J52:MJA109, J52:MJA185, and J52:MJA199 all show similar lifetime values, consistent with the similar TRMC profiles shown in figure 8. Sample 1 has the highest slow lifetime which corroborates well with the high mobilities of P3HT:N2200 blends in literature. Looking at the magnitude of the slow and fast components (A_2 and A_1 respectively) Samples S1, S5 and S6 have the longest fraction and correspondingly the lowest fraction for the fast component. The slow decay in these materials, is likely related to the stability of the materials as well as corroborated by the ageing tests performed.

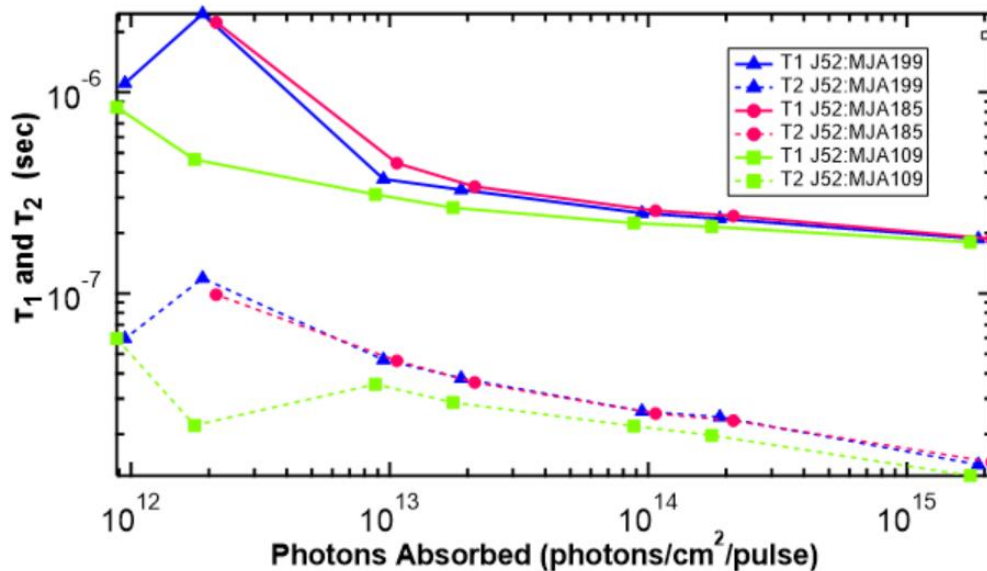


Figure 9. Lifetime parameters τ_1 (slow) and τ_2 (fast) extracted from the TRMC transients for the three new all-polymer blends as a function of light intensity.

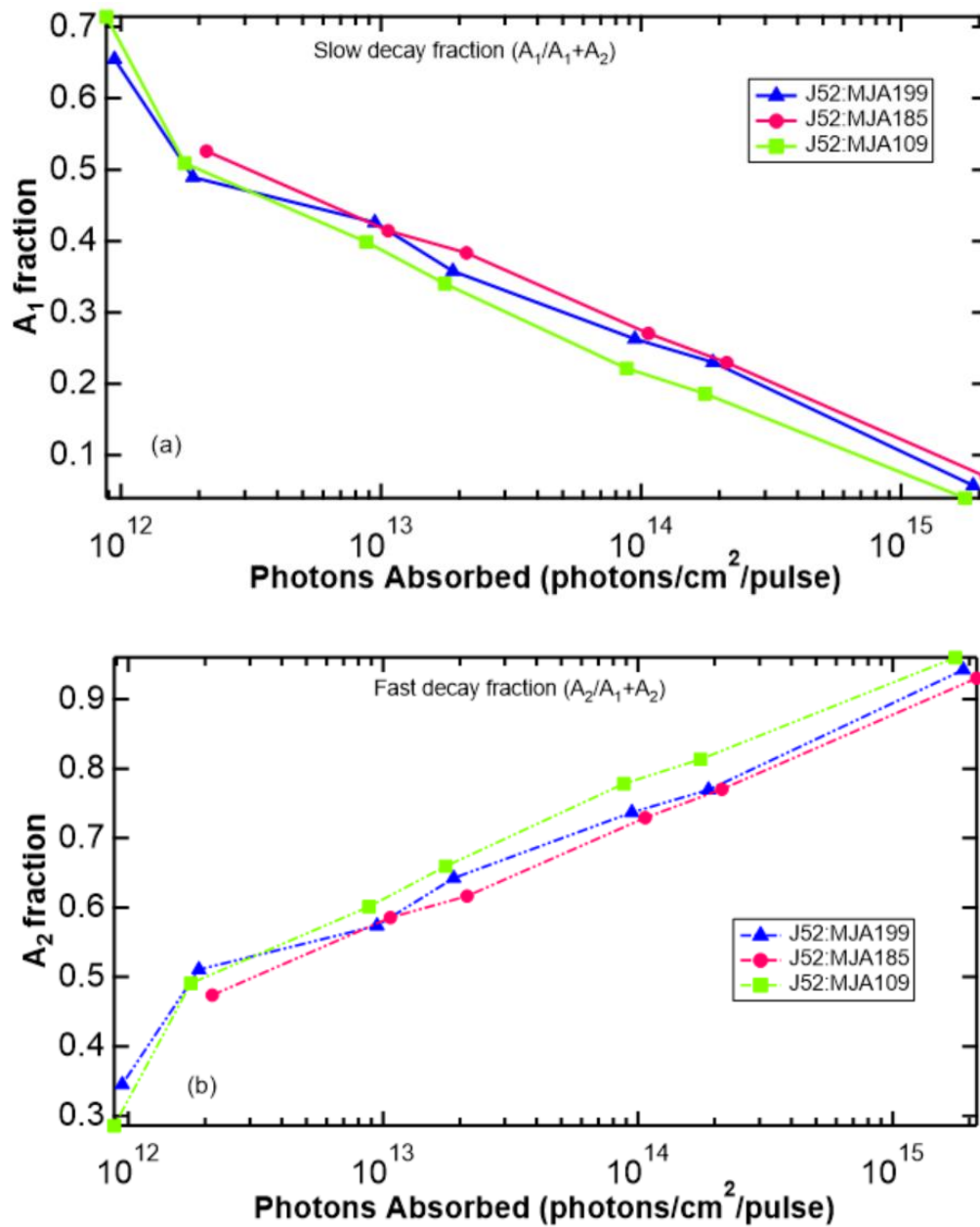


Figure 10. Contribution of the (a) slow and (b) fast component of the transient TRMC signal as a function of light intensity for the three new all-polymer blends.

Conclusions

The performance and TRMC response of eight all-polymer solar cell systems has been characterised. A strong positive and near linear correlation between cell short circuit current and $\phi\Sigma\mu$ peak signal was confirmed for all-polymer cells. A threshold $\phi\Sigma\mu$ peak signal of 0.06 cm²/Vs is recommended for screening new material combinations. The TRMC response of three new all-polymer systems, J52:MJA109, J52:MJA185, and J52:MJA199, were also analysed. Similar short-circuit currents were realised in devices consistent with the similar $\phi\Sigma\mu$ peak signals measured. Analysis of their lifetime confirm similar lifetimes for these systems.

Acknowledgements

This Activity received funding from ARENA as part of ARENA's Research and Development Program – Solar PV Research, project number 2017/RND0014, “Bringing All-Polymer Solar Cells Closer to Commercialization.” The views expressed herein are not necessarily the views of the Australian Government, and the Australian Government does not accept responsibility for any information or advice contained herein. Young-hun Shin and Michael Sommer of Chemnitz University of Technology are thanked for provision of 2S-N2200.

References

1. Cui, Y.; Yao, H.; Zhang, J.; Zhang, T.; Wang, Y.; Hong, L.; Xian, K.; Xu, B.; Zhang, S.; Peng, J.; Wei, Z.; Gao, F.; Hou, J., Over 16% efficiency organic photovoltaic cells enabled by a chlorinated acceptor with increased open-circuit voltages. *Nat. Commun.* **2019**, *10*, 2515.
2. Yuan, J.; Zhang, Y.; Zhou, L.; Zhang, G.; Yip, H.-L.; Lau, T.-K.; Lu, X.; Zhu, C.; Peng, H.; Johnson, P. A.; Leclerc, M.; Cao, Y.; Ulanski, J.; Li, Y.; Zou, Y., Single-Junction Organic Solar Cell with over 15% Efficiency Using Fused-Ring Acceptor with Electron-Deficient Core. *Joule* **2019**, *3*, 1140-1151.
3. Blom, P. W. M.; Mihailetschi, V. D.; Koster, L. J. A.; Markov, D. E., Device Physics of Polymer:Fullerene Bulk Heterojunction Solar Cells. *Adv. Mater.* **2007**, *19*, 1551-1566.
4. Li, G.; Zhu, R.; Yang, Y., Polymer solar cells. *Nat. Photon.* **2012**, *6*, 153-161.
5. McNeill, C. R.; Greenham, N. C., Conjugated-Polymer Blends for Optoelectronics. *Adv. Mater.* **2009**, *21*, 3840 - 3850.
6. Hou, J.; Inganäs, O.; Friend, R. H.; Gao, F., Organic solar cells based on non-fullerene acceptors. *Nat. Mater.* **2018**, *17*, 119.
7. Wang, G.; Melkonyan, F. S.; Facchetti, A.; Marks, T. J., All-Polymer Solar Cells: Recent Progress, Challenges, and Prospects. *Angewandte Chemie International Edition* **2019**, *58*, 4129-4142.
8. Savenije, T. J.; Ferguson, A. J.; Kopidakis, N.; Rumbles, G., Revealing the Dynamics of Charge Carriers in Polymer:Fullerene Blends Using Photoinduced Time-Resolved Microwave Conductivity. *J. Phys. Chem. C* **2013**, *117*, 24085-24103.
9. Oosterhout, S. D.; Kopidakis, N.; Owczarczyk, Z. R.; Braunecker, W. A.; Larsen, R. E.; Ratcliff, E. L.; Olson, D. C., Integrating theory, synthesis, spectroscopy and device efficiency to design and characterize donor materials for organic photovoltaics: a case study including 12 donors. *J. Mater. Chem. A* **2015**, *3*, 9777-9788.
10. Moore, J. R.; Albert-Seifried, S.; Rao, A.; Massip, S.; Watts, B.; Morgan, D. J.; Friend, R. H.; McNeill, C. R.; Siringhaus, H., Polymer Blend Solar Cells Based on a High-Mobility Naphthalenediimide-Based Polymer Acceptor: Device Physics, Photophysics and Morphology. *Adv. Energy Mater.* **2011**, *1*, 230-240.
11. Huang, W.; Li, M.; Lin, F.; Wu, Y.; Ke, Z.; Zhang, X.; Ma, R.; Yang, T.; Ma, W.; Liang, Y., Rational design of conjugated side chains for high-performance all-polymer solar cells. *Mol. Syst. Des. Eng.* **2018**, *3*, 103-112.

12. Deshmukh, K. D.; Prasad, S. K. K.; Chandrasekaran, N.; Liu, A. C. Y.; Gann, E.; Thomsen, L.; Kabra, D.; Hodgkiss, J. M.; McNeill, C. R., Critical Role of Pendant Group Substitution on the Performance of Efficient All-Polymer Solar Cells. *Chem. Mater.* **2017**, *29*, 804-816.
13. Li, Z.; Xu, X.; Zhang, W.; Meng, X.; Ma, W.; Yartsev, A.; Inganäs, O.; Andersson, M. R.; Janssen, R. A. J.; Wang, E., High Performance All-Polymer Solar Cells by Synergistic Effects of Fine-Tuned Crystallinity and Solvent Annealing. *J. Am. Chem. Soc.* **2016**, *138*, 10935-10944.
14. Rundel, K.; Shin, Y.-h.; Chesman, A. S. R.; Liu, A. C. Y.; Welford, A.; Thomsen, L.; Sommer, M.; McNeill, C. R., Effect of Thionation on the Performance of PNDIT2-Based Polymer Solar Cells. *J. Phys. Chem. C* **2019**, *123*, 12062-12072.